Inorganic Chemistry

Article

pubs.acs.org/IC

# Multicomponent Assembly of Anionic and Neutral Decanuclear Copper(II) Phosphonate Cages

Vadapalli Chandrasekhar,* Loganathan Nagarajan, Sakiat Hossain, Kandasamy Gopal,† Surajit Ghosh, and Sandeep Verma

Department of Chemistry, Indian Institute of Technology, Kanpur, Kanpur, 208016, India

Supporting Information

**ABSTRACT:** A multicomponent synthetic strategy involving copper(II) ions, *tert*-butylphosphonic acid ($t$-$BuPO_3H_2$) and 3-substituted pyrazole ligands has been adopted for the synthesis of soluble molecular copper(II) phosphonates. The use of six different 3-substituted pyrazoles, 3-R-PzH [R = H, Me, $CF_3$, Ph, 2-pyridyl (2-Py), and 2-methoxyphenyl (2-MeO-$C_6H_4$)] as ancillary ligands afforded nine different decanuclear cages, $[Cu_5(\mu_3\text{-}OH)_2(O_3P\text{-}t\text{-}Bu)_3(3\text{-}R\text{-}Pz)_2(X)_2]_2\cdot(Y)$ where R = H, X = $t$-$BuPO_3H$, and Y = $(Et_3NH^+)_4$(solvent) (**1**); R = Me, X = 3-MePzH, and Y = solvent (**2**); R = Me, X = $t$-$BuPO_3H$, and Y = $(Et_3NH^+)_4$(solvent) (**3**); R = $CF_3$, X = $t$-$BuPO_3H$, and Y = $(Et_3NH^+)_4$(solvent) (**4**); R = Ph, X = 3-PhPzH, and Y = solvent (**5**); R = 2-Py, X = 0.5 MeOH, and Y = solvent (**6**); R = 2-Py, X = none, and Y = solvent (**7**); R = 2-Py, X = $H_2O$, and Y = $(Et_3NH^+\cdot PF_6^-)_2$(solvent) (**8**); R = 2-MeO-$C_6H_4$, X = MeOH or 0.5:0.5 MeOH/$H_2O$, and Y = solvent (**9**). Compounds **1**–**6**, **8**, and **9** were isolated using a direct synthetic method which involves the reaction of copper(II) salts and the ligands, while **7** was obtained from an indirect route involving the reaction of preformed copper-pyridylpyrazolate precursor complexes and $t$-$BuPO_3H_2$. The decametallic compounds **1**–**9** possess a butterfly shaped core. The core of the cages **1**, **3**, and **4** are tetraanionic and contain more phosphonates than pyrazole ligands, while the other cages are neutral and contain more pyrazoles than phosphonate ligands. Compounds **1**–**6** have been studied by electrospray ionization-high-resolution mass spectrometry (ESI-HRMS). The decanuclear cage **6** was shown to be a good plasmid modifier.

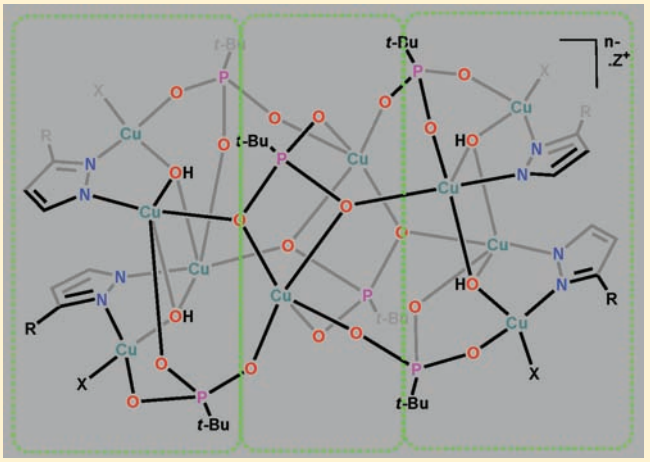


## INTRODUCTION

The last few decades witnessed many significant discoveries based on multinuclear metal cages such as several interesting magnetic materials including single molecule magnets (SMM).[1] Therefore, developing new and reliable synthetic strategies to assemble such cages are of considerable interest. Although phosphonate ligands are of potential utility in the construction of multinuclear metal assemblies, they received relatively limited attention due to the fact that metal complexes obtained from them are generally insoluble owing to possessing extended (1D, 2D, and 3D) structures.[2−5] The latter are important materials in their own right having potential applications in various fields including storage,[3] sorption,[4] and catalysis.[5] The preparation of zero-dimensional (0D) soluble multinuclear metal cages by the use of phosphonate ligands can be achieved by adopting novel synthetic strategies such as using sterically hindered phosphonic acids and/or using ancillary ligands which prevent formation of coordination polymers and assist in the isolation of lipophilic molecular compounds.[6] In addition to the challenge of preparing zero-dimensional molecular phosphonate cages, another formidable challenge is to be able to assemble cages with definite nuclearities. Thus, while a certain synthetic method might afford a molecular cage, often it is difficult in practice to generalize and prepare other analogues of such compounds even when the transition metal ion is kept the same.[6−9] We have been endeavoring in our efforts to (a) find synthetic methods that allow us to modulate the nuclearity of the cage and (b) to utilize such approaches in a general manner so that libraries of such compounds can be prepared. While, these goals have not been fully realized, we have been able to show that by a judicious choice of reaction conditions including variation in the type of phosphonates and the ancillary ligands, the nuclearity of Cu(II) phosphonates could be varied from 2 to 16.[9] However, thus far, particularly with high-nuclearity Cu(II) cages, we have not been able to access general synthetic protocols. In this paper, for the first time, we are able to demonstrate the efficacy of a synthetic procedure that allowed us to isolate as many as nine different Cu(II) phosphonate cages with structurally similar decanuclear cores. To our

**Received:** November 22, 2011
**Published:** May 10, 2012

   dx.doi.org/10.1021/ic202510d | *Inorg. Chem.* 2012, 51, 5605−5616

knowledge, this is the first time that such a general synthetic strategy has been successfully employed not only in Cu(II) phosphonates but among any family of multinuclear transition metal phosphonate cages.

Accordingly, the reaction of various Cu(II) salts with *t*-$BuPO_3H_2$ along with 3-substituted pyrazoles as coligands, 3-R-PzH (R = H, Me, $CF_3$, Ph, 2-Py, and 2-MeO-$C_6H_4$) afforded the decanuclear cages, $[Cu_5(\mu_3\text{-}OH)_2(O_3P\text{-}t\text{-}Bu)_3(3\text{-}R\text{-}Pz)_2(X)_2]_2\cdot(Y)$ where R = H, X = *t*-$BuPO_3H$, and Y = $(Et_3NH^+)_4$(solvent) (**1**); R = Me, X = 3-MePzH, and Y = solvent (**2**); R = Me, X = *t*-$BuPO_3H$, and Y = $(Et_3NH^+)_4$(solvent) (**3**); R = $CF_3$, X = *t*-$BuPO_3H$, and Y = $(Et_3NH^+)_4$(solvent) (**4**); R = Ph, X = 3-PhPzH, and Y = solvent (**5**); R = 2-Py, X = 0.5 MeOH, and Y = solvent (**6**); R = 2-Py, X = none, and Y = solvent (**7**); R = 2-Py, X = $H_2O$, and Y = $(Et_3NH^+\cdot PF_6^-)$(solvent) (**8**); R = 2-MeO-$C_6H_4$, X = MeOH or 0.5:0.5 MeOH/$H_2O$, and Y = solvent (**9**). The decametallic core of the three cages **1**, **3**, and **4** are anionic, and the remaining six are neutral. The synthesis and structure and a representative plasmid-modification capability of one of these cages (**6**) is reported here.

## EXPERIMENTAL SECTION

**Reagents and Instrumentation.** Solvents and other general reagents used in this work were purified according to standard procedures.[10a,b] The following chemicals were used as obtained. $Cu(ClO_4)_2\cdot 6H_2O$, $Cu_2(O_2CMe)_4\cdot 2H_2O$, anhydrous $Cu(SO_3CF_3)_2$, pyrazole (Fluka, Switzerland), $Cu(NO_3)_2\cdot 3H_2O$, $CuSO_4\cdot 5H_2O$ (NICE Chemicals, Cochin, India), $KPF_6$, anhydrous $CuCl_2$, *N*,*N*-dimethylformamide dimethylacetal, 2-acetylpyridine, 3-methylpyrazole (Aldrich), $AlCl_3$, $PCl_3$, and hydrazine hydrate 99% (SD Fine, India), supercoiled pBR322 plasmid DNA (Bangalore Genei), ethidium bromide (Sigma-Aldrich), magnesium monoperoxyphthalate hexahydrate (MMPP) (Lancaster, U.K.), sodium cacodylate buffer (SRL, Mumbai, India), ethylenediaminetetraacetic acid (EDTA), dimethyl sulfoxide (DMSO), *t*-butanol and D-mannitol (SD Fine, India). All buffer solutions were prepared using Millipore water. *t*-$BuPO_3H_2$[10c] and 3-(2-Py)-PzH[10d] were prepared by following the published procedures. A procedure similar to that used for preparing 3-(2-Py)-PzH has been used for the synthesis of 3-$CF_3$-PzH, 3-PhPzH, and 3-(2-MeO-$C_6H_4$)-PzH. Preparative procedures and structures for the {$Cu^{II}$-(3-(2-Py)-Pz)} precursor compounds are given in the Supporting Information.[11] Melting points were measured using a JSGW apparatus and are uncorrected. Elemental analyses were carried out by using a Thermo quest CE instrument model EA/110 CHNS-O elemental analyzer. $^1$H NMR was recorded on a JEOL-JNM LAMBDA 400 model NMR spectrometer in $CDCl_3$ solutions. The chemical shifts are referenced with respect to $SiMe_4$. Infrared (IR) spectra were recorded as KBr pellets on a Bruker Vector 22 Fourier transform (FT) IR spectrophotometer operating from 400 to 4000 $cm^{-1}$. High-resolution electrospray ionization-mass spectrometry (ESI-HRMS) spectra were recorded on a Micromass QUATTRO II triple quadrupole mass spectrometer for compounds **1**–**6**. For all the compounds, methanol was used as the solvent; the source and desolvation temperature was kept at 80 and 200 °C, respectively. The ESI-HRMS spectra were recorded under both positive and negative full scan mode (only positive mode was used for **5**). In all the cases, 2–5 $\mu$L of sample in methanol solvent was injected into the ionizing chamber and nitrogen gas was used for desolvation. The following ionization protocols were used. For **1**, the capillary voltage was maintained at 2.5 kV and the cone voltage was kept at 31.0 V, the extraction and ion guide voltages was kept at 1.2 and 0.9 kV, respectively. For **2**, **4**, and **6**, the capillary voltage was maintained at 2.2 kV, and the cone voltage was kept at 32.0 V for positive mode and 2.3 kV and 34.0 V for negative ion mode. The extraction voltage was maintained at 1.2 kV, and the ion guide voltage was maintained at 0.8 kV for positive ion mode while for the negative mode it was maintained at 1.0 and 1.3 kV, respectively. For **3**, the capillary voltage was maintained at 2.3 kV, and the cone voltage was kept at 34.0 V for positive mode and 2.2 kV and 32.0 V for negative ion mode (in acetonitrile solvent). For **5**, the capillary voltage was maintained at 2.44 kV and the cone voltage was kept at 32.0 V; the extraction cone voltage and ion guide voltage were maintained at 0.8 kV and 0.9 kV, respectively.

**Syntheses. 1**: A solution of PzH (0.004 g, 0.059 mmol), *t*-$BuPO_3H_2$ (0.008 g, 0.059 mmol), and $Et_3N$ (0.025 mL, 0.177 mmol) in MeOH (20 mL) was added dropwise to the MeCN (10 mL) solution of anhydrous $Cu(CF_3SO_3)_2$ (0.021 g, 0.059 mmol). The reaction mixture was stirred at room temperature for 16 h and filtered. The filtrate was kept for crystallization by slow diffusion of EtOAc at room temperature. Deep-blue crystals of **1** were obtained after 45 days. Yield: 0.004 g (24%). Anal. Calcd (%) for $[Et_3NH^+]_4[Cu_5(\mu_3\text{-}OH)_2(O_3P\text{-}t\text{-}Bu)_3(Pz)_2(t\text{-}BuPO_3H)_2^{2-}]_2\cdot(MeOH)_2(H_2O)_2$: C, 32.92; H, 6.59; N, 5.91. Found: C, 33.00; H, 6.72; N, 5.80. ESI-HRMS (*m*/*z*): 1189.16 [M/2 + $H_2O$ + 3H]$^-$, 1125.25 [M/2 − (*t*-Bu) + 2 + $H_2O$]$^-$. UV–vis (DCM/MeOH, $\lambda_{max}$/nm ($\varepsilon_{max}$/$M^{-1}$ $cm^{-1}$)): 618.5 (578.1). IR (KBr, $\nu$/$cm^{-1}$): 3776 (m, br), 3433 (m, br), 2977 (s), 2947 (s) 2740 (m), 2604 (m), 2531 (s), 2497(s), 2359 (s), 1633 (m, br), 1479 (s), 1446 (s), 1398 (s), 1360 (s), 1172 (m), 1077 (m), 1031 (s), 963 (m, br), 851 (m, br), 832 (m, br), 807 (w, br), 657 (s), 537 (s).

**2**: A solution of 3-MePzH (0.072 g, 0.874 mmol), *t*-$BuPO_3H_2$ (0.060 g, 0.437 mmol) and $Et_3N$ (0.123 mL, 0.874 mmol) in DCM (20 mL) was added dropwise to the MeOH (10 mL) solution of $Cu(ClO_4)_2\cdot 6H_2O$ (0.162 g, 0.437 mmol). The reaction mixture was stirred at room temperature for 16 h and filtered. Removal of solvent from the filtrate *in vacuo* afforded bluish green solid which was recrystallized from 1:1 mixture of DCM-MeOH to afford blue crystals of **2** in 15 days. Yield: 0.066 g (70%). Anal. Calcd (%) for $[Cu_5(\mu_3\text{-}OH)_2(O_3P\text{-}t\text{-}Bu)_3(3\text{-}MePz)_2(3\text{-}MePzH)_2]_2\cdot(MeOH)_4(CH_2Cl_2)_2$: C, 30.14; H, 4.98; N, 9.07. Found: C, 30.02; H, 5.09; N, 8.93. ESI-HRMS (*m*/*z*): 2172.84 [M]$^+$, 1085.92 [M/2]$^+$. UV–vis (DCM/MeOH, $\lambda_{max}$/nm ($\varepsilon_{max}$/$M^{-1}$ $cm^{-1}$)): 632.8 (700.56). IR (KBr, $\nu$/$cm^{-1}$): 3202 (s, br), 3064 (m, br), 2945 (br), 2861 (m, br), 2398 (br), 1807 (m), 1601 (s), 1462 (s), 1389 (s), 1344 (s), 1235 (s), 1134(s), 1073 (s), 957(s), 832 (s), 808 (s), 785(s), 660 (s), 559 (s), 502(s).

**3**: A solution of 3-MePzH (0.008 g, 0.099 mmol), *t*-$BuPO_3H_2$ (0.014 g, 0.099 mmol) and $Et_3N$ (0.04 mL, 0.287 mmol) in MeCN (20 mL) was added dropwise to the MeCN (10 mL) solution of anhydrous $CuCl_2$ (0.020 g, 0.149 mmol). The reaction mixture was stirred at room temperature for 40 h and filtered. Removal of solvent from the filtrate *in vacuo* afforded bluish green solid which was recrystallized from a 1:1 mixture of DCM–MeOH to afford blue crystals of **3** in 20 days. Yield: 0.029 g (69%). Anal. Calcd (%) for $[Et_3NH^+]_4[Cu_5(\mu_3\text{-}OH)_2(O_3P\text{-}t\text{-}Bu)_3(3\text{-}MePz)_2(t\text{-}BuPO_3H)_2]_2\cdot(MeOH)_8(H_2O)_2$: C, 34.16; H, 7.10; N, 5.43; P, 10.01. Found: C, 34.27; H, 7.22; N, 5.30. ESI-HRMS (*m*/*z*): 1163.26 [M-(*t*-Bu)]/2 − 3H]$^-$. IR (KBr, $\nu$/$cm^{-1}$): 3467 (m, br), 2999 (s), 2974 (s), 2763 (m), 2621 (m), 2552 (s), 2507 (s), 2371 (s), 1654 (m, br), 1488 (s), 1456 (s), 1409 (s), 1378 (s), 1185 (m), 1079 (s), 963 (m, br), 837 (m, br), 813 (m, br), 793 (m, br), 664 (s), 565 (s), 509 (s).

**4**: A solution of 3-$CF_3$-PzH (0.031 g, 0.226 mmol), *t*-$BuPO_3H_2$ (0.0312 g, 0.226 mmol) and $Et_3N$ (0.10 mL, 0.678 mmol) in MeCN (10 mL) was added dropwise to the solution of anhydrous $CuCl_2$ (0.046 g, 0.339 mmol) in MeCN (30 mL). The reaction mixture was stirred at room temperature for 20 h and filtered. Removal of solvent from the filtrate *in vacuo* afforded bluish green solid which was recrystallized from a 1:1 mixture of DCM–MeOH to afford blue crystals of **4** in 20 days. Yield: 0.069 g (72%). Anal. Calcd (%) for $[Et_3NH^+]_4[Cu_5(\mu_3\text{-}OH)_2(O_3P\text{-}t\text{-}Bu)_3(3\text{-}CF_3\text{-}Pz)_2(t\text{-}BuPO_3H)_2]_2\cdot(MeOH)_3(H_2O)_3$: C, 31.47; H, 5.98; N, 5.31. Found: C, 31.73; H, 6.11; N, 5.01. ESI-HRMS (*m*/*z*): 1426.05 [M/2 − $Et_3NH$ + $H_2O$ + 2]$^-$. IR (KBr, $\nu$/$cm^{-1}$): 2960 (m, br), 2930 (m, s), 2869 (m, br), 1550 (s, br), 1481 (s), 1455 (m), 1430 (s), 1379 (m), 1360 (m), 1224 (s), 1079 (s), 991 (m, br), 893 (s, br), 884 (s), 829 (s), 774 (s), 642 (s), 617 (s), 554 (s).


dx.doi.org/10.1021/ic202510d | *Inorg. Chem.* 2012, 51, 5605–5616

**Table 1. Crystal Data for Compounds 1−3 and 7−9**

| compound | 1 | 2 | 3 | 7 | 8 | 9 |
|---|---|---|---|---|---|---|
| formula | $C_{76}H_{172}Cu_{10}N_{12}O_{34}P_{10}$ | $C_{56}H_{98}Cu_{10}N_{16}O_{22}P_6$ | $C_{56}H_{110}Cu_{10}N_8O_{34}P_{10}$ | $C_{58}H_{86}Cl_4Cu_{10}N_{12}O_{22}P_6$ | $C_{56}H_{88}Cu_{10}F_{7.97}N_{12}O_{26}P_8$ | $C_{134}H_{198}Cu_{20}N_{16}O_{58}P_{12}$ |
| formula weight | 2743.46 | 2168.83 | 2384.73 | 2266.51 | 2380.11 | 4603.74 |
| crystal system | triclinic | triclinic | triclinic | monoclinic | monoclinic | triclinic |
| space group | $P\bar{1}$ | $P\bar{1}$ | $P\bar{1}$ | $P2(1)/c$ | $C2/m$ | $P\bar{1}$ |
| temperature (K) | 100(2) | 100(2) | 273(2) | 100(2) | 100(2) | 100(2) |
| $a$ (Å) | 14.4554(16) | 11.4076(10) | 15.331(4) | 12.0048(18) | 21.5813(18) | 13.044(3) |
| $b$ (Å) | 15.6368(17) | 16.2503(14) | 15.885(5) | 25.105(4) | 24.4312(18) | 16.077(4) |
| $c$ (Å) | 16.3618(19) | 16.3249(11) | 18.275(5) | 15.954(2) | 10.8552(9) | 26.441(7) |
| $\alpha$ (deg) | 98.349(2) | 116.225(3) | 65.916(5) | 90 | 90 | 80.781(5) |
| $\beta$ (deg) | 113.954(2) | 104.829(3) | 69.997(5) | 106.272(2) | 115.620(2) | 77.499(5) |
| $\gamma$ (deg) | 97.686(2) | 99.540(3) | 67.706(5) | 90 | 90 | 67.090(4) |
| volume (Å$^3$) | 3267.2(6) | 2485.0(3) | 3665.9(18) | 4615.6(12) | 5160.8(7) | 4969(2) |
| $Z$ | 1 | 1 | 1 | 2 | 2 | 1 |
| reflns coll./unique | 18466/12589 | 13143/8799 | 24008/12944 | 25270/9071 | 17279/6597 | 25072/17520 |
| $R_{int}$ | 0.0529 | 0.0361 | 0.0677 | 0.0669 | 0.0499 | 0.0579 |
| data/restraints/params | 12589/3/652 | 8799/0/582 | 12944/408/580 | 9071/2/522 | 6597/15/289 | 17520/0/1107 |
| goodness-of-fit on $F^2$ | 0.911 | 1.049 | 0.824 | 1.023 | 1.185 | 0.941 |
| final $R$ indices $[I > 2\sigma(I)]^a$ | $R_1$ = 0.0692 | $R_1$ = 0.0626 | $R_1$ = 0.0678 | $R_1$ = 0.0612 | $R_1$ = 0.0632 | $R_1$ = 0.0713 |
| | $wR_2$ = 0.1525 | $wR_2$ = 0.1358 | $wR_2$ = 0.1857 | $wR_2$ = 0.1486 | $wR_2$ = 0.1662 | $wR_2$ = 0.1573 |
| $R$ indices (all data)$^a$ | $R_1$ = 0.1308, | $R_1$ = 0.0799, | $R_1$ = 0.1320, | $R_1$ = 0.0946, | $R_1$ = 0.0915, | $R_1$ = 0.1190, |
| | $wR_2$ = 0.1777 | $wR_2$ = 0.1451 | $wR_2$ = 0.2088 | $wR_2$ = 0.1615 | $wR_2$ = 0.2106 | $wR_2$ = 0.1786 |
| largest residuals (e.Å$^{-3}$) | 1.626 and −0.696 | 1.480 and −0.554 | 0.645 and −0.552 | 0.925 and −0.958 | 1.601 and −1.576 | 0.976 and −0.798 |

$^a R_1 = \Sigma||F_0| - |F_c||/\Sigma|F_0|$; $wR_2 = \{[\Sigma w(|F_0|^2|F_c|^2)^2]/[\Sigma w(|F_0|^2)^2]\}^{1/2}$.



dx.doi.org/10.1021/ic202510d | Inorg. Chem. 2012, 51, 5605−5616

**5**: A solution of 3-PhPzH (0.032 g, 0.224 mmol), *t*-$BuPO_3H_2$ (0.016 g, 0.112 mmol) and $Et_3N$ (0.04 mL, 0.224 mmol) in DCM (20 mL) was added dropwise to the solution of anhydrous $CuCl_2$ (0.015 g, 0.112 mmol) in MeOH (10 mL). The reaction mixture was stirred at room temperature for 16 h and filtered. Removal of solvent from the filtrate *in vacuo* afforded bluish green solid, which was recrystallized from a 1:1 mixture of DCM−MeOH to afford greenish blue crystals of **5** in 15 days. Yield: 0.012 g (20%). Anal. Calcd (%) for $[Et_3NH^+]_4[Cu_5(\mu_3\text{-}OH)_2(O_3P\text{-}t\text{-}Bu)_3(3\text{-}PhPz)_2(3\text{-}PhPzH)_2]_2\cdot(H_2O)_2$: C, 46.28; H, 6.02; N, 9.00. Found: C, 45.97; H, 6.19; N, 9.12. ESI-HRMS (*m*/*z*): 1068.05 $\{[(M - (3\text{-}PhPzH)_2)/2] + H_2O + 3H\}^+$, 966.02 $\{[(M - (3\text{-}PhPzH)_2)/2] - Ph - 3H\}^+$. UV−vis (DCM/MeOH, $\lambda_{max}$/nm ($\varepsilon_{max}$/$M^{-1}$ $cm^{-1}$)): 700.45 (612.58). IR (KBr, $\nu$/$cm^{-1}$): 2962 (m, br), 2923 (m), 2832 (m, br), 1576 (s), 1557 (s), 1521 (m), 1491 (s), 1459 (m), 1417 (s), 1375 (m), 1363 (m), 1225 (m), 1022 (s), 997 (s), 969 (m, br), 894 (s), 837 (s, br), 785 (s), 665 (s), 605 (s), 546 (m).

**6**:[9b] A solution of 2-Py-3-PzH (0.017 g, 0.117 mmol), *t*-$BuPO_3H_2$ (0.016 g, 0.117 mmol) and $Et_3N$ (0.065 mL, 4.70 mmol) in DCM (20 mL) was added dropwise to the solution of $Cu(ClO_4)_2\cdot 6H_2O$ (0.087 g, 0.235 mmol) in DCM (30 mL). The reaction mixture was stirred at room temperature for 20 h and filtered. The blue precipitate obtained was recrystallized from a 2:1 mixture of DCM−MeOH to afford the deep-blue crystals of **6** in 10 days. Yield: 0.020 g (41%). Anal. Calcd (%) for $[Cu_5(\mu_3\text{-}OH)_2(O_3P\text{-}t\text{-}Bu)_3(3\text{-}(2\text{-}Py)\text{-}Pz)_2(MeOH)]_2\cdot(MeOH)_{10}(H_2O)_2$: C, 32.38; H, 5.27; N, 6.76. Found: C, 32.12; H, 5.41; N, 6.67. ESI-HRMS (*m*/*z*): 2060.76 $[M - (t\text{-}Bu + (MeOH)_2)) + H_2O + 2H]^+$, 1064.90 $[(M/2) - (CH_3OH + 1) + H_2O]^+$. UV−vis (DCM/MeOH, $\lambda_{max}$/nm ($\varepsilon_{max}$/$M^{-1}cm^{-1}$)): 648.2 (556.98). IR (KBr, $\nu$/ $cm^{-1}$): 3525 (s, br), 2968 (s), 2868 (m), 2015 (m, br), 1613 (s), 1476 (m), 1453 (m), 1367(m), 1161 (m, br), 833 (m), 776 (s). Compound **6** can also be synthesized by using $Cu_2(O_2CMe)_4\cdot 2H_2O$, anhydrous $Cu(CF_3SO_3)_2$, anhydrous $CuCl_2$, $Cu(NO_3)_2\cdot 3H_2O$, $CuSO_4\cdot 5H_2O$, or $Cu(BF_4)_2\cdot xH_2O$ in the place of $Cu(ClO_4)_2\cdot 6H_2O$. $Cu(BF_4)_2\cdot xH_2O$ could be synthesized *in situ* using anhydrous $CuCl_2$ and anhydrous $Li(BF_4)_2$ in MeOH.

**7**: A solution of *t*-$BuPO_3H_2$ and $Et_3N$ was added dropwise to the solution of the {Cu-(3-(2-Py)-Pz)} preformed cage. The reaction mixture was stirred at room temperature for 20 h and filtered. Removal of solvent from the filtrate *in vacuo* afforded blue-green solid which was recrystallized from the 2:1 mixture of DCM−MeOH to afford dark blue crystals of **7** in 15 days. Five different {Cu-(3-(2-Py)-Pz)} preformed cage precursors were employed for the synthesis of **7**. The specific details for each reaction as follows. (a) *t*-$BuPO_3H_2$ (0.035 g, 0.252 mmol) and $Et_3N$ (0.065 mL, 0.470 mmol) in DCM (20 mL); $[Cu(O_2C\text{-}Me)(3\text{-}(2\text{-}Py)\text{-}Pz)]_n$ (0.112 g, 0.420 mmol) in a 2:1 mixture of DCM−MeOH (30 mL). Yield: 0.036 g (41%). (b) *t*-$BuPO_3H_2$ (0.016 g, 0.117 mmol) and $Et_3N$ (0.065 mL, 0.47 mmol) in DCM (20 mL); $[Cu(3\text{-}(2\text{-}Py)\text{-}Pz)(3\text{-}(2\text{-}Py)\text{-}Pz)(ClO_4)]_2$ (0.168 g, 0.186 mmol) in MeOH (30 mL). Yield: 0.028 g (36%). (c) *t*-$BuPO_3H_2$ (0.026 g, 0.186 mmol) and $Et_3N$ (0.12 mL, 0.93 mmol) in DCM (20 mL); $[Cu_2(3\text{-}(2\text{-}Py)\text{-}Pz)_2(NO_3)_2(H_2O)_2]$ (0.214 g, 0.372 mmol) in MeOH (30 mL). Yield: 0.065 g (42%). (d) *t*-$BuPO_3H_2$ (0.0202 g, 0.146 mmol) and $Et_3N$ (0.10 mL, 0.73 mmol) in DCM (20 mL); $[Cu_4(3\text{-}(2\text{-}Py)\text{-}Pz)_6(ClO_4)_2]$ (0.391 g, 0.292 mmol) in MeOH (30 mL). Yield: 0.0992 g (40%). (e) *t*-$BuPO_3H_2$ (0.021 g, 0.152 mmol) and $Et_3N$ (0.08 mL, 0.61 mmol) in DCM (20 mL); $[Cu_4(3\text{-}(2\text{-}Py)\text{-}Pz)_6\cdot(NO_3)_2]$ (0.304 g, 0.245 mmol) in MeOH (30 mL). Yield: 0.092 g (45%). Anal. Calcd (%) for $[Cu_5(\mu_3\text{-}OH)_2(O_3P\text{-}t\text{-}Bu)_3(3\text{-}(2\text{-}Py)\text{-}Pz)_2]_2\cdot(CH_2Cl_2)_8(H_2O)_4$: C, 27.07; H, 3.48; N, 5.92. Found: C, 27.44; H, 3.59; N, 5.79. UV−vis (DCM/MeOH, $\lambda_{max}$/nm ($\varepsilon_{max}$/$M^{-1}$ $cm^{-1}$)): 648.11 (556.35). IR (KBr, $\nu$/$cm^{-1}$): 3534 (s, br), 2976 (s), 2878 (m), 2021 (br), 1619 (s), 1489 (m), 1464 (m), 1377(m), 1171 (m, br), 846 (m), 786 (s).

**8**: 3-(2-Py)-PzH (0.019 g, 0.194 mmol) and *t*-$BuPO_3H_2$ (0.016 g, 0.117 mmol) was added portionwise to the solution of anhydrous $CuCl_2$ (0.044 g, 0.324 mmol) in MeOH (30 mL) with constant stirring. Solid $KPF_6$ (0.130 g 0.72 mmol) was added to the above reaction mixture and continued to be stirred for 1 h. Then $Et_3N$ (0.12 mL, 0.862 mmol) was then added, and the reaction mixture was stirred at room temperature for another 16 h and filtered. DCM (15 mL) was added to the above filtrate kept for crystallization by slow evaporation at room temperature. Deep-blue crystals of **8** were obtained after 25 days. Yield: 0.040 g (46.7%). Anal. Calcd (%) for $[Cu_5(\mu_3\text{-}OH)_2(O_3P\text{-}t\text{-}Bu)_3(3\text{-}(2\text{-}Py)\text{-}Pz)_2(OH_2)_2]_2\cdot(Et_3NH^+\cdot PF_6^-)_2(MeOH)$: C, 27.49; H, 3.80; N, 6.75. Found: C, 30.89; H, 4.61; N, 7.39. IR (KBr, $\nu$/$cm^{-1}$): 2953 (m, br), 2926 (m), 2828 (m), 1574 (m), 1568 (s), 1505 (m), 1487 (s), 1458 (m), 1415 (s), 1375 (m), 1363 (m), 1226 (m), 1022 (s), 993 (s), 964 (m), 893 (s), 833 (s), 785 (s), 662 (s), 605 (s).

**9**: A solution of $Cu(ClO_4)_2\cdot 6H_2O$ (0.087 g, 0.235 mmol), *t*-$BuPO_3H_2$ (0.016 g, 0.117 mmol) and $Et_3N$ (0.065 mL, 4.70 mmol) in MeOH (30 mL) was stirred for 4 h to form a green colored turbid solution. A solution of 3-(2-MeO-$C_6H_4$)-PzH (0.020 g, 0.117) in DCM (10 mL) was added dropwise to the above mixture and stirred for a further 8 h. The clear reaction mixture was filtered, concentrated, and left for slow evaporation to afford blue crystals of **9** in 20 days. Yield: 0.020 g (41%). Anal. Calcd (%) for $[Cu_5(\mu_3\text{-}OH)_2(O_3P\text{-}t\text{-}Bu)_3(3\text{-}(2\text{-}MeO\text{-}C_6H_4)\text{-}Pz)_2(MeOH)_2]_2\cdot(MeOH)_4(H_2O)$: C, 34.77; H, 5.19; N, 4.51. Found: C, 34.75; H, 5.24; N, 4.55. UV−vis (DCM/MeOH, $\lambda_{max}$/nm ($\varepsilon_{max}$/$M^{-1}$ $cm^{-1}$)): 691 (575.43). IR (KBr, $\nu$/$cm^{-1}$): 3472 (s, br), 2968 (m), 2944.48 (m), 2863 (s, br), 1608 (s), 1583 (s), 1522 (s), 1388 (m), 1175 (s), 1141 (s), 1071 (s), 1051 (s), 981 (s), 753 (s).

**X-ray Crystallography.** Data were collected on Bruker APEX II CCD diffractometer ($MoK_\alpha$, $\lambda$ = 0.710 73 Å). Complete hemispheres of data were collected using $\omega$-scans (0.3°, up to 30 s/frame). Integrated intensities were obtained with SAINT+,[12a] and when they were corrected for absorption SADABS was used.[12b] Structure solution and refinement was performed with the SHELXTL-package.[12c] The structures were solved by direct methods and completed by iterative cycles of DF syntheses and full-matrix least-squares refinement against $F^2$.[12d] The thermal parameters of two carbon atoms (C35B and C36B) in **1** were nonpositive definite and were hence refined isotropically. All the other non-hydrogen atoms were refined with anisotropic displacement parameters. All the hydrogen atoms on the carbon frameworks were included in the final stages of the refinement and were refined with a typical riding model. The asymmetric unit of **1**−**3** and **7**−**9** contained severely disordered solvent molecules, two $Et_3NH^+$ units in **3**, and two $Et_3NH^+$ unit in **8**. These could not be modeled satisfactorily. Therefore the PLATON/"SQUEEZE" program[12e] was used to remove such disordered units from the respective overall intensity data. The details of the squeezed electron density are appended to the respective cif files. Details of the data collection and refinement parameters are given in Table 1. CCDC 726181 (**1**), 726179 (**2**), 726182 (**3**), 272462 (**6**), 726177 (**7**), 726178 (**8**), and 834797 (**9**) contain the supplementary crystallographic data for this paper. These data can be obtained free of charge at www.ccdc.cam.ac.uk/conts/retrieving.html [or from the Cambridge Crystallographic Data Centre, 12, Union Road, Cambridge CB2 1EZ, U.K. Fax: +44-1223/336-033. E-mail: deposit@ccdc.cam.ac.uk].

**pBR322 Cleavage Assay.** Plasmid cleavage reactions were performed with the use of sodium cacodylate buffer (10 mM, pH 7.5, 32 °C) containing pBR322 (8 $\mu$g/mL, Bangalore Genei) solution of **6** (1 mM) in distilled DMSO and activating agents magnesium monoperoxyphthalate (MMPP, 100 $\mu$M). For each cleavage reaction, 16−18 $\mu$L of pBR322 supercoiled DNA and 2 $\mu$L of the solution of **6** was used and were initiated by adding 2 $\mu$L of MMPP in an Eppendorf tube. For scavenger experiments, the concentrations used were 100 mM. All cleavage reactions were quenched with 5 $\mu$L of loading buffer containing 100 mM of EDTA and 50% glycerol in Tris−HCl (pH 8.0) and the samples were loaded onto 0.7% agarose gel (Biozym) containing ethidium bromide (1 $\mu$g/mL). Electrophoresis was done for 1 h at constant current (80 mA) in 0.5× TBE buffer. Gels were imaged with a PC-interfaced Bio-Rad Gel Documentation System 2000.

**Plasmid Cleavage under Anaerobic Conditions.** Oxygen-free nitrogen was bubbled through cacodylate buffer, which was then subjected to four freeze−thaw cycles. All reagents were transferred in an argon filled glovebag, and Eppendorf tubes were tightly sealed with parafilm in the argon atmosphere. Reactions were quenched with


dx.doi.org/10.1021/ic202510d | *Inorg. Chem.* 2012, 51, 5605−5616

**Scheme 1. Synthesis of Compounds 1−5**

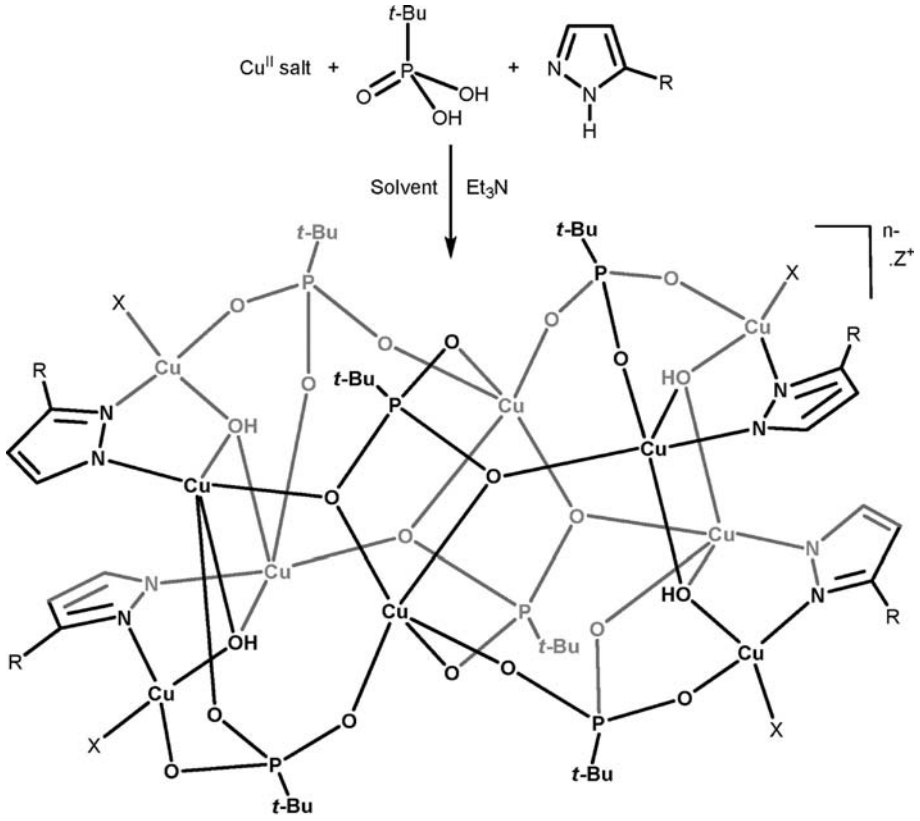


| Cu$^{II}$ salt | R | X | n- | Z$^+$ | |
|---|---|---|---|---|---|
| anhydrous $Cu(CF_3SO_3)_2$ | H | [*t*-BuPO$_3$H]$^-$ | 4- | 4 Et$_3$NH$^+$ | (**1**) |
| $Cu(ClO_4)_2{\cdot}6H_2O$ | Me | 3-MePzH | 0 | - | (**2**) |
| anhydrous $CuCl_2$ | Me | [*t*-BuPO$_3$H]$^-$ | 4- | 4 Et$_3$NH$^+$ | (**3**) |
| anhydrous $CuCl_2$ | $CF_3$ | [*t*-BuPO$_3$H]$^-$ | 4- | 4 Et$_3$NH$^+$ | (**4**) |
| anhydrous $CuCl_2$ | Ph | 3-PhPzH | 0 | - | (**5**) |

loading buffer and efforts were made to ensure strict anaerobic conditions during irradiation and quenching.

## RESULTS AND DISCUSSION

**Synthetic Aspects.** The reaction of anhydrous $Cu(CF_3SO_3)_2$ with *t*-BuP(O)(OH)$_2$ and pyrazole (1:1:1) in the presence of 3 equiv of triethylamine afforded the tetraanionic decanucler copper(II) cage **1** (Scheme 1). Similarly, the reaction of anhydrous $CuCl_2$, *t*-BuPO$_3$H$_2$, and 3-MePzH/3-$CF_3$PzH (1.5:1:1 ratio) in the presence of Et$_3$N also produced the tetraanionic decanucler copper(II) cages **3** and **4** (Scheme 1). In contrast, an analogous reaction involving 3-MePzH but using 2 equiv (1:1:2 ratio) afforded the neutral decanuclear cage **2** (Scheme 1). The reduction of the amount of triethylamine in the reaction leading to the formation of **2** clearly inhibits formation of excess [*t*-BuP(O)$_2$(OH)]$^-$. As a result, neutral pyrazole ligands occupy the peripheral coordination on copper atoms. The use of 3-PhPzH (1:1:2 ratio) also produces a neutral decanuclear cage **5** (Scheme 1). Likewise, the reaction involving the pyrazole with a coordinating substituent, 3-(2-Py)-PzH, (2:1:1 ratio) also leads to the formation of a neutral decanuclear cage **6** (Scheme 2). The latter was previously reported by us in a preliminary communication.[9b] The yield of **6** could be optimized and increased to as much as ∼80% by carrying out the reaction according to the crystal structure stoichiometry (5 equiv of $Cu(ClO_4)_2{\cdot}6H_2O$, 2 equiv of 3-(2-Py)-PzH, 3 equiv of *t*-BuPO$_3$H$_2$, and a slight excess of Et$_3$N). The formation of **6** is quite general, and the reaction of various other Cu(II) salts such as $Cu_2(O_2CMe)_4{\cdot}2H_2O$, anhydrous $Cu(CF_3SO_3)_2$, anhydrous $CuCl_2$, $Cu(NO_3)_2{\cdot}3H_2O$, $CuSO_4{\cdot}5H_2O$, or $Cu(BF_4)_2{\cdot}xH_2O$ in the place of $Cu(ClO_4)_2{\cdot}6H_2O$ also afforded **6**.

The use of preformed copper(II) complexes (di- and higher nuclearity) in cluster-expansion reactions is not well-practiced, although in the case of iron and manganese phosphonates this is well-known. Thus, the compound $[M^{II/III}{}_3O(O_2C\text{-}R)_6L_3]^{0/+1}$ (M = Mn or Fe; R = Me, *t*-Bu, or Ph; L = solvents) have been conveniently used to prepare several multinuclear phosphonates.[6−9] Recently, we had used a dinuclear copper complex and predictably expanded it to a tetranuclear cage by replacement of acetate bridging groups by phosphonate bridging units.[9i] Spurred by this, we reacted preformed copper-pyridylpyrazole complexes, such as $[Cu(O_2CMe)(3\text{-}(2\text{-Py})\text{-Pz})]_n$, $[Cu(3\text{-}(2\text{-Py})\text{-Pz})(3\text{-}(2\text{-Py})\text{-PzH})(ClO_4)]_2$, $[Cu_2(3\text{-}(2\text{-Py})\text{-Pz})_2{\cdot}(NO_3)_2{\cdot}(H_2O)_2]$, $[Cu_4(3\text{-}(2\text{-Py})\text{-Pz})_6{\cdot}(ClO_4)_2]$, or $[Cu_4(3\text{-}(2\text{-Py})\text{-Pz})_6{\cdot}(NO_3)_2]$ with *t*-


dx.doi.org/10.1021/ic202510d | Inorg. Chem. 2012, 51, 5605−5616

**Scheme 2. Synthesis of Compounds 6–9**

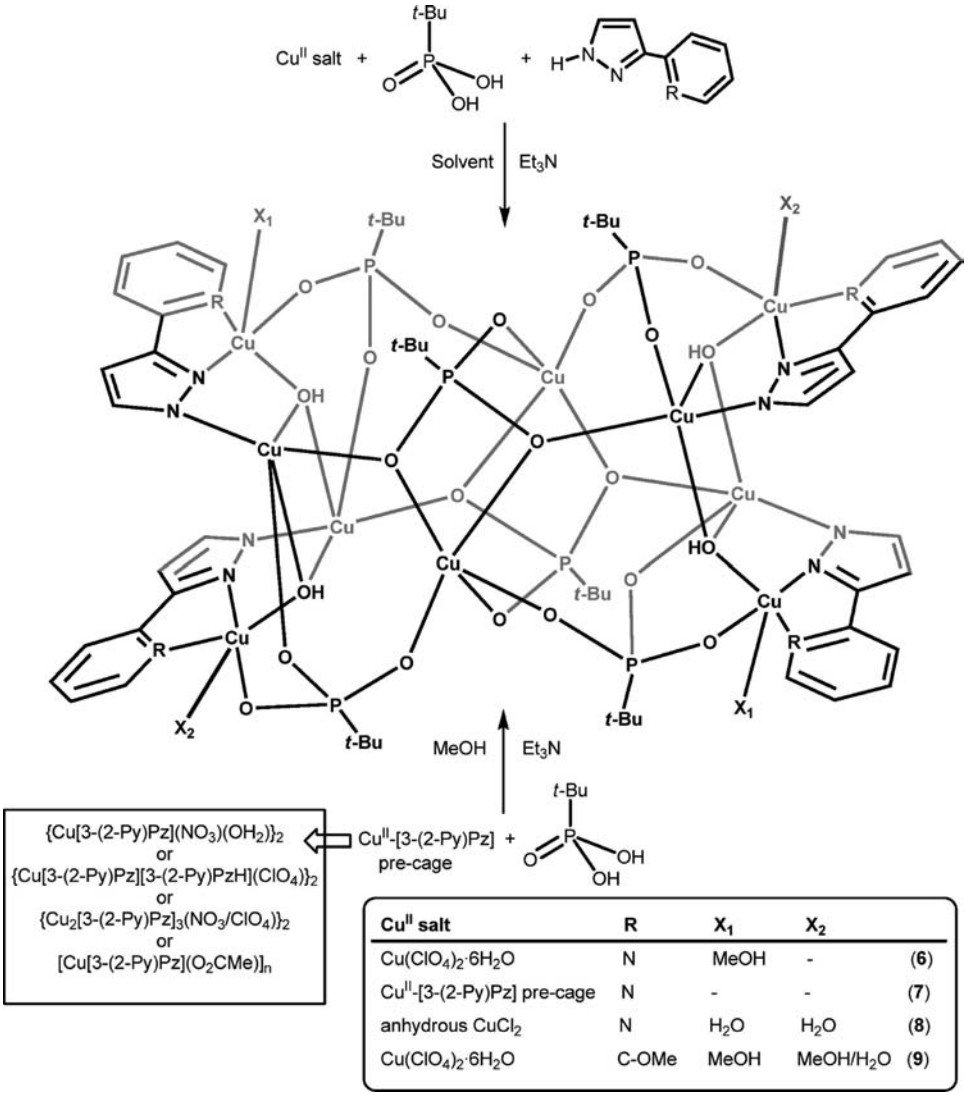


| Cu$^{II}$ salt | R | X$_1$ | X$_2$ | |
|---|---|---|---|---|
| Cu(ClO$_4$)$_2$·6H$_2$O | N | MeOH | - | (**6**) |
| Cu$^{II}$-[3-(2-Py)Pz] pre-cage | N | - | - | (**7**) |
| anhydrous CuCl$_2$ | N | H$_2$O | H$_2$O | (**8**) |
| Cu(ClO$_4$)$_2$·6H$_2$O | C-OMe | MeOH | MeOH/H$_2$O | (**9**) |

$BuPO_3H_2$ in the presence of $Et_3N$. All of these reactions afforded the cage **7**, where the two peripheral copper(II)–solvent (MeOH) coordinations in **6** are removed (Scheme 2). The isolation of **7** in all of these reactions suggests the rich dividends that are possible by a judicious choice of preformed copper(II) cages in Cu(II) phosphonate cage chemistry. We were also interested in examining if a copper(II) salt with a bulky noncoordinating counteranion can be an effective starting material. Accordingly, we used *in situ* generated $Cu(PF_6)_2$ and were able to isolate cage **8**, where all the four peripheral copper(II) atoms in **6** and **7** are found in coordination with water molecules (Scheme 2). Also, cage **8** contained $Et_3NH^+ \cdot PF_6^-$ units in its crystal lattice. Finally, we chose 3-(2-MeO-$C_6H_4$)-PzH as the coligand with the intention of exploring whether a mild coordinating unit in the form of the -OMe group would alter the course of the reaction. Evidently, the tendency of formation of the decanuclear cage is so strong in these situations (cage **9**) that the peripheral copper(II) ions accepts coordination from the weakly coordinating -OMe group to maintain its structural integrity (Scheme 2).

**Molecular Structures of 1–3 and 6–9.** The molecular structures of a large number of cages prepared herein have been established by single crystal X-ray diffraction analysis. Although, the core structure of **5** could be established, the poor quality of X-ray data precluded a complete solution of the structure. Also, we were unable to isolate appropriate crystals of **4** and hence its structure could not be determined from X-ray diffraction. However, ESI-HRMS studies on **4** (see below) reveal peaks due to one-half of the molecule. For all the other compounds, the molecular structures could be unambiguously established by single crystal X-ray diffraction analysis. Irrespective of whether the cage is anionic or neutral, their broad structural features are quite similar as described below.

The molecular structures of cages **1–3** and **6–9** reveal that they are all structurally analogous decanuclear cages (Figure 1). All these cages possess a butterfly shaped $\{Cu_{10}P_6\}$ core. Cages **1–3**, **6**,[9b] and **9** crystallized in the triclinic system ($P\bar{1}$ space group, $Z = 1$), while **7** and **8** crystallized in the monoclinic system ($P2_1/c$ and $C2/m$ space groups, respectively, $Z = 2$). The asymmetric unit of all these cages contains half the molecule, except **8** where one-fourth of the molecule was present. Structural analyses of all the compounds reveals that the 10 copper atoms present in the cage are bound together by four $\mu_3$-OH, four anionic pyrazolates (3-R-$Pz^-$) and six dianionic phosphonate ligands ($t$-$BuPO_3^{2-}$). In addition, either four monoanionic phosphonate ligands ($t$-$BuPO_3H^-$ in **1**, **3**,


dx.doi.org/10.1021/ic202510d | *Inorg. Chem.* 2012, 51, 5605–5616

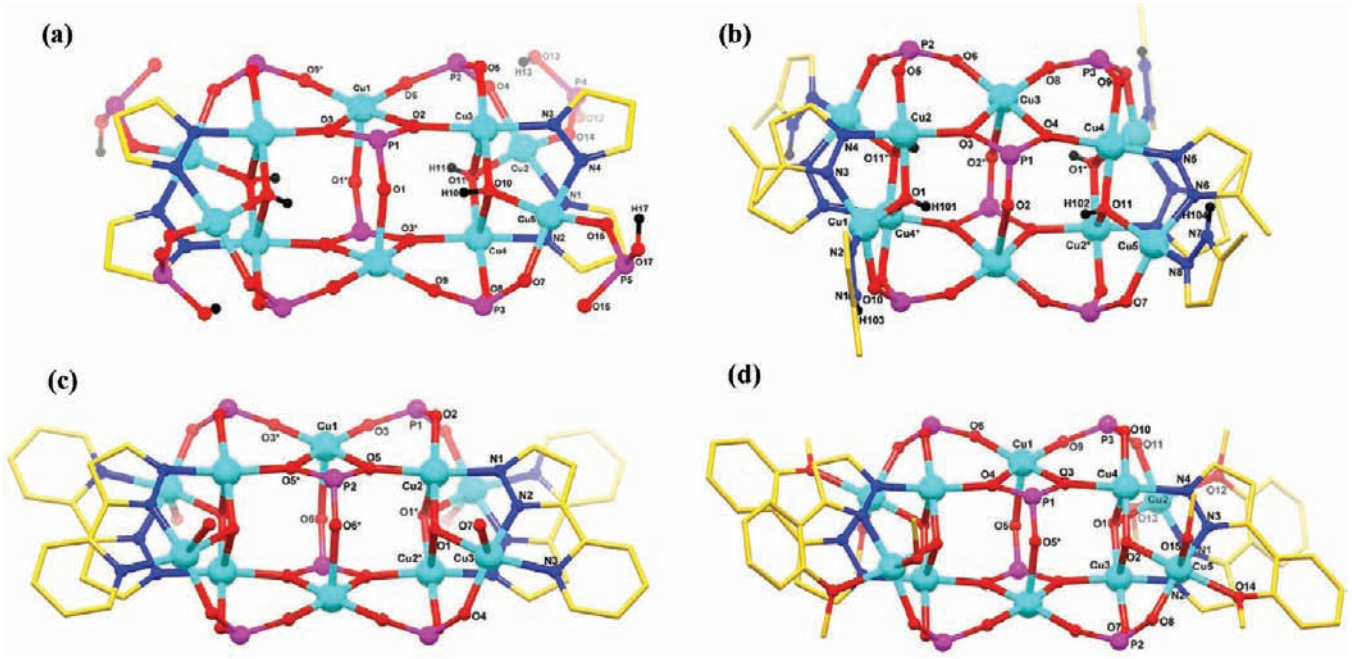


**Figure 1.** Molecular structures of **1** (a), **2** (b), **8** (c), and **9** (d). Unlabeled atoms are symmetry related to labeled atoms (*). All the hydrogen atoms (except OH and NH) and *t*-butyl groups on each phosphorus are removed for clarity. Selected bond parameters are given in the Supporting Information.

and **4**) or four neutral pyrazole ligands (3-R-PzH in **2**, R = Me and **5**, R = Ph) are found in coordination with copper(II) centers present in the periphery of the cages. In **1**, **3**, and **4** four $Et_3NH^+$ units per cage are found in the crystal lattice for charge neutrality. While in **8**, two $[E_3NH^+ \cdot PF_6^-]$ units are also found in the crystal lattice along with the $\{Cu_{10}P_6\}$ cage. Although cages **1**−**5** are structurally analogous with each other, cages **1**, **3**, and **4** contain more phosphonates than pyrazole ligands while cages **2** and **5** contain more pyrazoles than phosphonate ligands. In other words, cages **2** and **5** represent the pyrazole rich assemblies while cages **1**, **3**, and **4** represent the phosphonate rich assemblies. However, in **1**−**5**, the peripheral $[t\text{-}BuPO_3H]^-$ or 3-R-PzH ligands are replaced by the pyridinic unit of the 3-(2-Py)-$Pz^-$ ligands (in **6**−**8**) or the -OMe group of the 3-(2-OMe-$C_6H_4$)-$Pz^-$ ligands (in **9**).

All the cages are built up of a structurally similar $\{Cu_{10}P_6\}$ core; the structure of **1** is used here as a representative example to illustrate the general structural features of these cages. The molecular structure of **1** (Figure 1a) reveals that the decanuclear cage is essentially composed of three discrete structural units: a dimeric central rim $\{Cu_2(O_3P\text{-}t\text{-}Bu)_2\}$, two diamond-shaped $\{Cu_2(\mu_3\text{-}OH)_2\}$ units, and two peripheral pairs of Cu(II) centers. The latter two units in unison could be termed as the wings of the cage while the central rim is the main body. It is interesting to note that only the peripheral copper(II) atoms (Cu2, Cu5, Cu2*, and Cu5*) of the wings possess the ancillary pyrazole ligands. The central rim copper atoms (Cu1 and Cu1*) are tightly bound by the coordination action of two [4.211] (Harris notation[13]) phosphonate ligands (P1 and P1*). It also connects the central rim portion to the diamond-shaped $\{Cu_2(\mu_3\text{-}OH)_2\}$ units at the wings (Cu3, Cu4, Cu3*, and Cu4*). The assistance of the $\mu_3$-OH bridges in connecting the diamond-shaped dimers to the peripheral pairs of copper atoms is clearly discernible.

Finally, two pairs of $[t\text{-}BuPO_3]^{2-}$ ligands (P2, P3, P2*, and P3*) help to stitch the body and wings, viz., central rim, the diamond-shaped copper pairs, and the peripheral copper atoms together with an [3.111] coordination. Because of this multiple coordination action involving the phosphonates, pyrazolates, and hydroxide ligands, multiple ring substructures result in the overall cage structure. Another interesting aspect of these cages are the remarkable variation in the coordination environment and coordination geometry around the copper(II) atoms (Table S1; Supporting Information). Each centrosymmetrically related subunit of the decanuclear cage contains four different types of copper atoms which are either four or five coordinate. It is interesting to correlate the structure of **1** with that of the hexadecanuclear copper(II) phosphonate cage, $[Cu_8(\mu_3\text{-}OH)_2(\mu\text{-}OH)_2(O_3P\text{-}t\text{-}Bu)_3(Pz)_4(O_2CMe)_2(MeCN)]_2$.[9g] It is clear that these two structural types share the common decanuclear butterfly motif. It is reasonable to assume that the decanuclear core of cage **1** is formed first and further elaboration through bicapping leads to the hexadecanuclear cage.

Other decanuclear cages formed in this study can also be described in a similar manner as that of **1**. Depending on the geometry and coordination, the copper(II) atoms present in the cages **1**−**9** can be classified into three or four types as summarized in Table S1 (Supporting Information). In all the cages, the central rim copper(II) atoms are five coordinate (5O coordination) with a square-pyramidal geometry, while the four copper(II) atoms present in each wing possess either four coordination (square-planar geometry) or five coordination (square-pyramidal geometry). The axial coordination of the square-pyramidal (five-coordinated) wing copper(II) atoms are derived from either neutral methanol or water molecules. Although a discussion on the bonding parameter of the cages **1**−**9** is not attempted here, it is clear that the overall trends found are not too dissimilar (see the Supporting Information). Further, all of these cages are truly nanodimensional. For example, the overall size of the **6** is ~20 × 15 × 10 Å$^3$, where the dimensions are measured between the protons lying on the


dx.doi.org/10.1021/ic202510d | *Inorg. Chem.* 2012, 51, 5605−5616

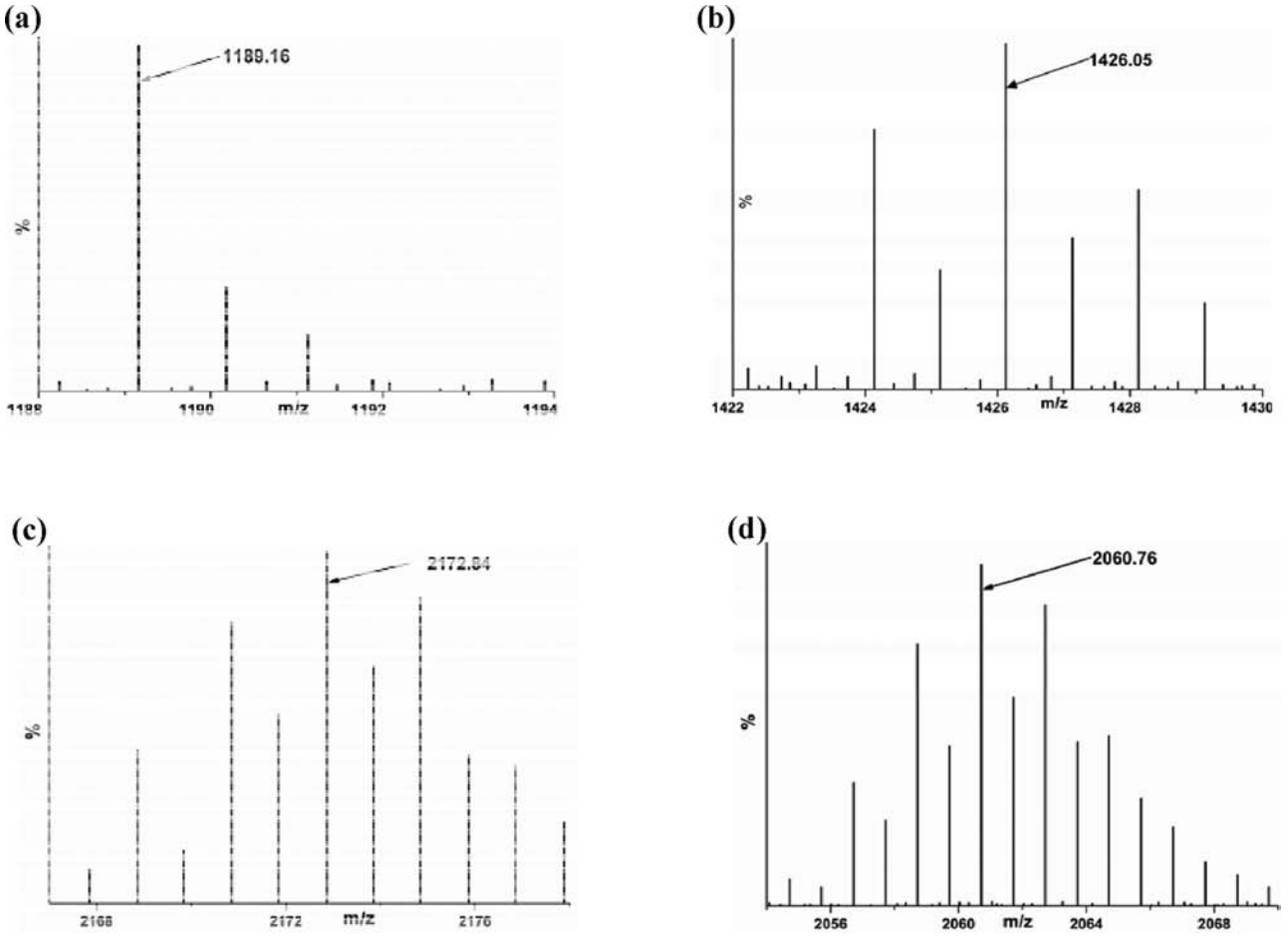


**Figure 2.** Isotopic distribution for $[M/2 + H_2O + 3H]^-$ of **1** (a), $[M/2 - Et_3NH + H_2O + 2H]^-$ of **4** (b), $[M]^+$ of **2** (c) and $[M - (t\text{-Bu} + (MeOH)_2) + H_2O + 2H]^+$ of **6** (d).

surface in all the sides.[9b] Interestingly, the presence of the $PF_6^-$ anion in the cage **8** leads to the formation of an interesting supramolecular architecture that is mediated through C−H---F interactions (see the Supporting Information).

**Solution Studies.** The question about the structural integrity of large molecular cages in solution is always intriguing. In order to resolve this question for the compounds reported in this study, pure crystals of compounds **1**−**6** were dissolved in methanol and their solution behavior was studied by ESI-HRMS, recorded under positive and negative ion modes. Two intense peaks seen at 1189.16 and 1125.25 for compound **1** are assigned to $[M/2 + H_2O + 3H]^-$ and $[M/2 - (t\text{-Bu}) + 2 + H_2O]^-$ ions, respectively, indicating the possibility of dissociation of the decanuclear core, in solution, to two identical halves (Figure 2a). Similarly, compound **3** shows a peak at 1163.26 assigned for the $\{[M - (t\text{-Bu})]/2 - 3H\}^-$ ion, and compound **4** shows a peak at $m/z$ = 1426.05 assigned for the $[M/2 - Et_3NH + H_2O + 2]^-$ ion (Figure 2b). Compound **5** shows two peaks at 1068.05 and 966.02 assigned for $\{[(M - (3\text{-PhPzH})_2)/2] + H_2O + 3H\}^+$ and $\{[(M - (3\text{-PhPzH})_2)/2] - Ph - 3H\}^+$ ions, respectively.

In contrast to the above, compound **2** shows two peaks at 2172.84 and 1085.92 assigned for $[M]^+$ (Figure 2c) and $[M/2]^+$ ions, respectively, while **6** shows two peaks at 2060.76 and 2078.78, assigned for $[M - (t\text{-Bu} + (MeOH)_2)) + H_2O + 2H]^+$ and $[M - (t\text{-Bu} + (MeOH)_2) + (H_2O)_2 + 2H]^+$ ions, respectively (Figure 2d). The molecular ion peaks observed for compounds **2** and **6** indicates the stability of the decanuclear core structure in solution (entire assembly of **2** and **6** remains intact). In addition, the other prominent peaks seen at 1064.91 and 1020.85 for compound **6** are assigned to $\{(M/2) - MeOH - 2H + H_2O\}^+$ and $\{[M - (MeOH)_2 - (t\text{-Bu})]/2\}^{2+}$ ions, respectively. From these data, it is clear that the structural integrity of the cages is retained in some cases while in the others the cage does not completely fall apart but seems to split into two equal halves.

Although it is difficult to predict the mechanism of the formation of high nuclearity cages, it is possible to offer some thoughts on their stepwise assembly[14] with the help of ESI-HRMS data. In view of the molecular structures of **1**−**13**, it is possible to postulate that species such as **A**−**F** (Scheme 3) may be the probable building blocks that are involved in their formation. Of these various species, $\mathbf{A_1}$, $\mathbf{B_1}$, $\mathbf{C_1}$, $\mathbf{D_1}$, $\mathbf{A_4}$, $\mathbf{B_4}$, $\mathbf{A_5}$, and $\mathbf{C_3}$ have been identified in the ESI-HRMS of **1**−**5**. Incidentally these species form the crucial building blocks of the wing part of the decanuclear cage. In addition, species **E** and **F** were identified in the ESI-HRMS of **6**−**8**. All the compounds show the existence of different species as summarized in Scheme 3; compounds **1**−**3** are used here as a representative example to explain the structural features. Thus, ion **C** was identified as either $[\mathbf{C_1}]^+$ ion ($m/z$ = 487.95) or a $[\mathbf{C_3} - H]^+$ ion ($m/z$ = 762.90) while the ions $\mathbf{A_1}$ ($[\mathbf{A_1} + H]^+$, $m/z$ = 563.02; $[\mathbf{A_1} + CH_3CO + H_2O]^+$, $m/z$ = 580.09), $\mathbf{A_4}$ ($[\mathbf{A_4} - 2OH + 2H]^+$, $m/z$ = 652.03; $[\mathbf{A_4} + CO - 3H]^+$, $m/z$ = 708.00),


dx.doi.org/10.1021/ic202510d | Inorg. Chem. 2012, 51, 5605−5616

**Scheme 3. Summary of Various Building Blocks Involved in the Formation of the Cages 1−6[a]**

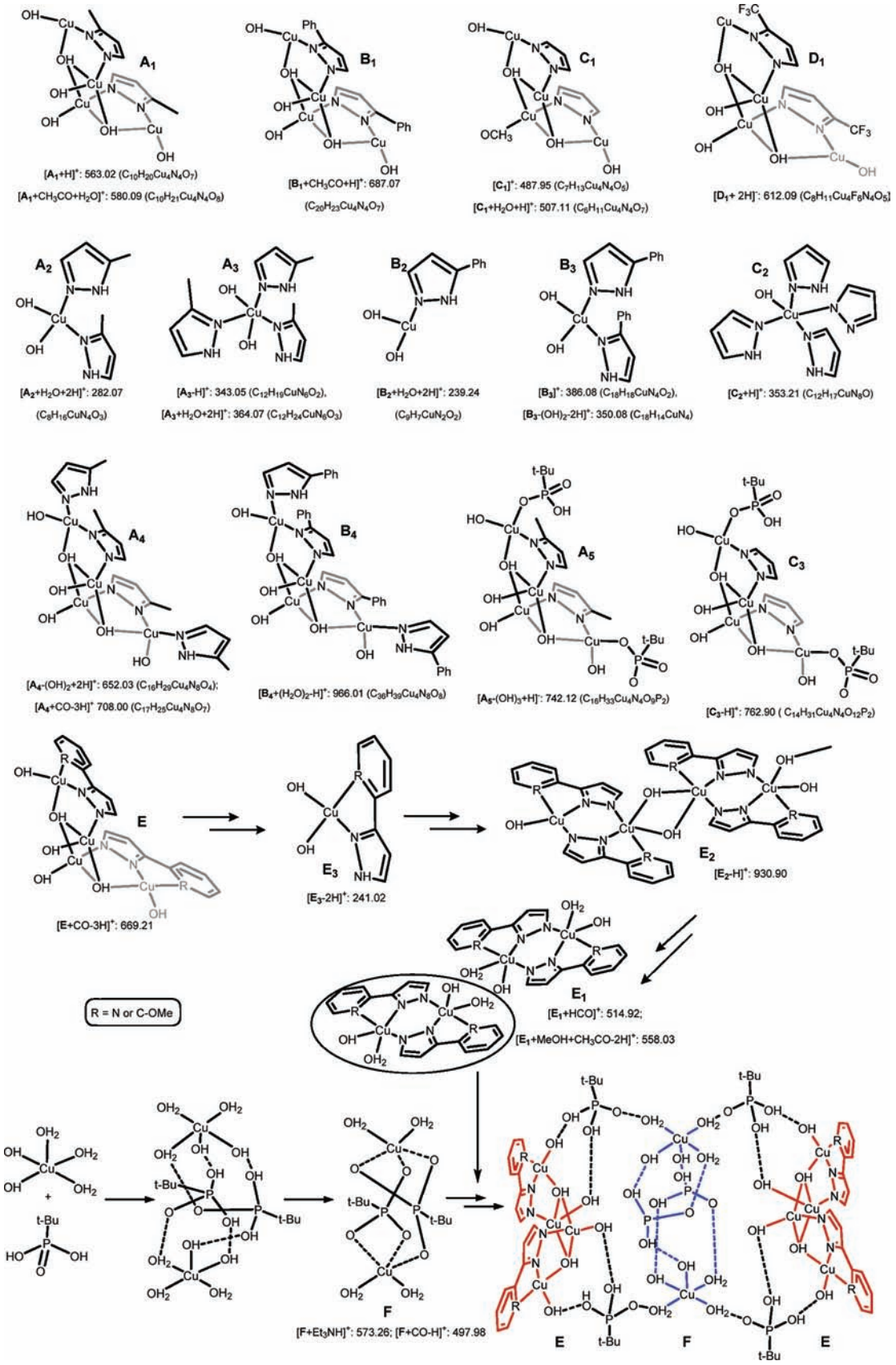


[a]A plausible mechanism for the *in situ* generated species **E**−$E_3$, **F**, and its conversion into cage **6** is also given.


dx.doi.org/10.1021/ic202510d | *Inorg. Chem.* 2012, 51, 5605−5616

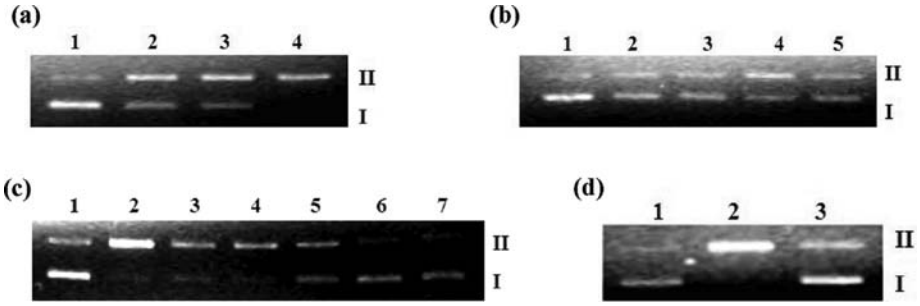


**Figure 3.** (a) Cage **6**-mediated pBR322 DNA cleavage experiments at different time intervals from form I to form II. Lane 1: DNA alone. Lanes 2–4: DNA + **6** (30, 60, and 90 min, respectively). (b) pBR322 DNA cleavage effected by **6** in the presence of MMPP at different time intervals. Lane 1: DNA alone. Lanes 2–5: DNA + **6** + MMPP (2, 5, 10, 15, and 20 min, respectively). (c) pBR322 DNA cleavage experiments assisted by **6** in the presence of free-radical scavengers and singlet oxygen quenchers in a 90 min reaction. Lane 1: DNA alone. Lane 2: pBR322 + **6**. Lane 3: pBR322 + 2.1 + DMSO. Lane 4: pBR322 + **6** + D-mannitol. Lane 5: pBR322 + 2.1 + *t*-BuOH. Lane 6: pBR322 + **6** + EDTA. Lane 7: pBR322 + **6** + $NaN_3$. (d) pBR322 DNA cleavage assisted by **6** in anaerobic conditions at different time intervals. Lane 1: DNA alone. Lanes 2 and 3: DNA + **6** and DNA + **6** under anaerobic conditions.

and $\mathbf{A_5}$ ($\mathbf{A_5}$ − 3OH + H]$^+$, $m/z$ = 742.12) are found to be present in the ESI-HRMS of **2** and **3**. A similar observation was also found for other cages.

We envisage the formation of the Cu(II)OH complex, $[Cu_2(OH)_2(3\text{-}(2\text{-}Py)\text{-}Pz)_2(H_2O)_2]$ ($\mathbf{E_1}$) from $\mathbf{E_2}$ or $\mathbf{E_3}$ under basic conditions (Scheme 3). Two molecules of $\mathbf{E_1}$ upon condensation would afford a tetrameric complex, $[Cu_4(OH)_4(3\text{-}(2\text{-}Py)\text{-}Pz)_4(MeOH)]$ ($\mathbf{E_2}$) (Scheme 3). Species such as $[Cu(OH)_2(3\text{-}(2\text{-}Py)\text{-}Pz)]$ ($\mathbf{E_3}$) is likely to be generated in solution which upon further rearrangement may lead to the species $[Cu_4(OH)_6(3\text{-}(2\text{-}Py)\text{-}Pz)_2]$ (**E**). Similarly, the copper-(II)-aqua salt and *t*-$BuPO_3H_2$ would react to generate $[Cu(t\text{-}BuPO_3)_2(H_2O)_4]$ (**F**). The combination of **E** and **F** with deprotonated phosphonates (*t*-$BuPO_3^{2-}$) could result in the formation of **6** (Scheme 3). The observed peaks at 514.92 correspond to the $\{\mathbf{E_1} + (HCO)\}^+$ ion, while the peak at 930.90 is assigned as the $\{\mathbf{E_2} - H\}^+$ ion. Similarly, a peak at 241.02 is assigned as the $[\mathbf{E_3} - 3H]^+$ ion where as the ion **E** is identified as its $CO^+$ adduct ($[\mathbf{E} + (CO) - 3H]^+$, $m/z$= 669.20). The ion **F** is observed as its $Et_3NH^+$ salt ($[\mathbf{F} + Et_3NH]^+$, $m/z$ = 573.26) and also as the $CO^+$ adduct ($[\mathbf{F} + (CO) - H]^+$, $m/z$ = 497.98). The $CO^+$ and $CH_3CO^+$ may be generated *in situ* under the mass spectral condition due to the presence of trace amounts of acetone in methanol solvent. Further confirmation on the stepwise formation of the decanuclear cages could come from an isolation of some, if not all, fragments suggested here. Such studies are being carried out.

**Plasmid-Cleavage Behavior of 6.** Transition metal complexes in general, and those of copper(II) in particular, are known to show nuclease activity. However, most of the studies known in literature have been carried out on mono, di, or trinuclear complexes.[9c,d,15] Metal complexes of nuclearity more than three have been very rarely studied for their nuclease acvity. Recently, we have demonstrated that multicopper(II) phosphonates (tetra- and dodecanuclear cages) are effective plasmid modifiers.[9f–h] In view of this, we chose to study the plasmid-modification capability of **6** as a representative example. The nuclease activity studies of **6** were carried out in DMSO solvent. Time course experiments revealed that 100% conversion of the supercoiled pBR322 DNA form I to nick form II occurs in 90 min in the presence of **6** (Figure 3a). To foster the reaction, magnesium monoperoxyphthalate (MMPP) was added upon which up to 50% conversion was observed only in 20 min (Figure 3b). The mechanism of the plasmid cleavage process was probed by several experiments. First, the crucial role of copper(II) ions is indicated by the complete inhibition of plasmid cleavage in the presence of EDTA (Figure 3c; lane 6). Copper(II) based artificial nucleases are known to cleave either through a hydrolytic or oxidative pathway. To probe the cleavage mechanism, hydroxyl radical scavengers such as DMSO, D-mannitol, and *t*-butylalcohol and the singlet oxygen quencher, $NaN_3$, were chosen. Some inhibition by *t*-BuOH is noted (Figure 3c; lane 5) while DMSO and D-mannitol did not inhibit the cleavage reactions (Figure 3c; lanes 3 and 4). On the other hand, $NaN_3$ effected a complete inhibition (Figure 3c; lane 7), indicating the lack of direct involvement of diffusible hydroxyl radicals. Molecular oxygen is the essential coreactant in oxidative processes. To probe its role, the reactions were performed under strictly anaerobic conditions. Interestingly, the DNA cleaving ability of **6** completely stopped under anaerobic conditions (Figure 3d). A requirement of dioxygen for the oxidative scission reaction is substantiated by the fact that no hydroxyl radical and no cleavage were observed under anaerobic conditions. A mechanistic model that is consistent with these observations has a diffusible metal ion-generated reactive oxygen species.

## ■ CONCLUSIONS

In conclusion, this report describes a series of structurally analogous decanuclear copper(II) phosphonate cages synthesized by a multicomponent synthetic strategy involving copper(II) salts, *t*-$BuPO_3H_2$ and 3-R-PzH [R = H, Me, $CF_3$, Ph, 2-pyridyl (2-Py), and 2-methoxyphenyl (2-MeO-$C_6H_4$)]. The role of 3-substituted pyrazoles and the reaction stoichiometry seem to be crucial for assembling the decanuclear cages. Compounds **1**–**9** possess a butterfly shaped core. The core of the decametallic cages **1**, **3**, and **4** are tetraanionic and contain more phosphonate than the pyrazole ligands, while the cages **2** and **5** are neutral and contain more pyrazoles than the phosphonate ligands. Compounds **1**–**6** have been studied by ESI-HRMS, and possible fragments involved in the construction of the cages have been identified. The decanuclear cage **6** was shown to be a good plasmid DNA modifier under native or added co-oxidant conditions.


dx.doi.org/10.1021/ic202510d | *Inorg. Chem.* 2012, 51, 5605–5616

## ■ ASSOCIATED CONTENT

### Supporting Information

X-ray data (CIF); synthesis of starting materials, additional figures, and tables (PDF). This material is available free of charge via the Internet at http://pubs.acs.org.

## ■ AUTHOR INFORMATION


### Corresponding Author

*E-mail: vc@iitk.ac.in.

### Present Address

[†]Department of Chemistry, Indian Institute of Technology, Bombay, Mumbai, 400076, India.


### Notes

The authors declare no competing financial interest.

## ■ ACKNOWLEDGMENTS

We thank the Department of Science and Technology (DST), India, for financial support including support for a Single Crystal CCD X-ray Diffractometer facility at IIT-Kanpur. V.C. is thankful to the DST for a J. C. Bose fellowship. S.V. is a Shri Devaraj Chair Professor at IIT-Kanpur. S.H. thanks the Council of Scientific and Industrial Research (CSIR), India, for a research fellowship (SRF), and K.G. is thankful to the DST for a SERC Fast Track Scheme for Young Scientists Project Fellowship. We thank Prof. Raymond J. Butcher, Department of Chemistry, Howard University, Washington, DC 20059 for his assistance in solving the structures during the revision stage. We also acknowledge Mr. Tapas Ghatak and Mr. Prem Lama, IIT Kanpur, for their help in X-ray crystallography.

## ■ REFERENCES


(1) (a) Sessoli, R.; Gatteschi, D.; Caneschi, A.; Novak, A. M. *Nature* **1993**, *365*, 141. (b) Sessoli, R.; Tsai, H.-L.; Schake, A. R.; Wang, S.; Vincent, J. B.; Folting, K.; Gatteschi, D.; Christou, G.; Hendrickson, D. N. *J. Am. Chem. Soc.* **1993**, *115*, 1804. (c) Blagg, R. J.; Muryn, C. A.; McInnes, E. J. L.; Tuna, F.; Winpenny, R. E. P. *Angew. Chem., Int. Ed.* **2011**, *50*, 6530. (d) Guo, Y.-N.; Xu, G.-F.; Wernsdorfer, W.; Ungur, L.; Guo, Y.; Tang, J.; Zhang, H.; Chibotaru, L. F.; Powell, A. K. *J. Am. Chem. Soc.* **2011**, *133*, 11948. (e) Feltham, H. L. C.; Clèrac, R.; Powell, A. K.; Brooker, S. *Inorg. Chem.* **2011**, *50*, 4232. (f) Feltham, H. L. C.; Lan, Y.; Klöwer, F.; Ungur, L.; Chibotaru, L. F.; Powell, A. K.; Brooker, S. *Chem.—Eur. J.* **2011**, *17*, 4362. (g) Colacio, E.; Ruiz-Sanchez, J.; White, F. J.; Brechin, E. K. *Inorg. Chem.* **2011**, *50*, 7268. (h) Rigaux, G.; Inglis, R.; Morrison, S.; Prescimone, A.; Cadiou, C.; Evangelisti, M.; Brechin, E. K. *Dalton Trans.* **2011**, *40*, 4797. (i) Habib, F.; Lin, P.−H.; Long, J.; Korobkov, I.; Wernsdorfer, W.; Murugesu, M. *J. Am. Chem. Soc.* **2011**, *133*, 8830. (j) Papatriantafyllopoulou, C.; Wernsdorfer, W.; Abboud, K. A.; Christou, G. *Inorg. Chem.* **2011**, *50*, 421. (k) Taguchi, T.; Wernsdorfer, W.; Abboud, K. A.; Christou, G. *Inorg. Chem.* **2010**, *49*, 10579. (l) Winpenny, R. E. P.; McInnes, E. J. L. Molecular Nanomagnets. In *Molecular Materials*; Bruce, D. W., O'Hare, D., Walton, R. I., Eds.; John Wiley & Sons Ltd., Chichester, U.K., 2010.

(2) (a) Clearfield, A. *Curr. Opin. Solid State Mater. Sci.* **2002**, *6*, 495. (b) Poojary, D. M.; Zhang, B.; Clearfield, A. *J. Am. Chem. Soc.* **1997**, *119*, 12550. (c) Clearfield, A. *Curr. Opin. Solid State Mater. Sci.* **1996**, *1*, 268. (d) Thompson, M. E. *Chem. Mater.* **1994**, *6*, 1168. (e) Subbiah, A.; Pyle, D.; Rowland, A.; Huang, J.; Narayanan, R. A.; Thiyagarajan, P.; Zoń, J.; Clearfield, A. *J. Am. Chem. Soc.* **2005**, *127*, 10826. (f) Song, S.-Y.; Ma, J.-F.; Yang, J.; Cao, M.-H.; Li, K.-C. *Inorg. Chem.* **2005**, *44*, 2140. (g) Ouellette, W.; Yu, M. H.; O'Connor, C. J.; Zubieta, J. *Inorg. Chem.* **2006**, *45*, 7628. (h) Sharma, C. V. K.; Clearfield, A. *J. Am. Chem. Soc.* **2000**, *122*, 4394. (i) Ouellette, W.; Yu, M. H.; O'Connor, C. J.; Zubieta, J. *Inorg. Chem.* **2006**, *45*, 3224. (j) Burkholder, E.; Golub, V.; O'Connor, C. J.; Zubieta, J. *Inorg. Chem.* **2004**, *43*, 7014. (k) *Metal Phosphonate Chemistry: From Synthesis to Applications*; Clearfield, A., Demadis, K., Eds.; Royal Society of Chemistry: Cambridge, U.K., 2012.

(3) (a) Alberti, G. *Acc. Chem. Res.* **1978**, *11*, 163. (b) Jaber, M.; Larlus, O.; Mieche-Brendle, J. *Solid State Sci.* **2007**, *9*, 144.

(4) (a) Fredoueil, F.; Massiot, D.; Janvier, P.; Gingl, F.; Bujoli-Doeuff, M.; Evian, M.; Clearfield, A.; Bujoli, B. *Inorg. Chem.* **1999**, *38*, 1831. (b) Maeda, K.; Kiyozumi, Y.; Mizukami, F. *J. Phys. Chem. B* **1997**, *101*, 4402. (c) Yue, Q.; Yang, J.; Li, G.-H.; Li, G.-D.; Chen, J.-S. *Inorg. Chem.* **2006**, *45*, 4431. (d) Gallagher, L. A.; Serron, S. A.; Wen, X.; Hornstein, B. J.; Dattelbaum, D. M.; Schoonover, J. R.; Meyer, T. J. *Inorg. Chem.* **2005**, *44*, 2089. (e) Maeda, K. *Microporous Mesoporous Mater.* **2004**, *73*, 47.

(5) (a) Wan, B. Z.; Anthony, R. G.; Peng, G. Z.; Clearfield, A. *J. Catal.* **1986**, *101*, 19. (b) Deniaud, D.; Schöllorn, B.; Mansuy, J.; Rouxel, J.; Battioni, P.; Bujoli, B. *Chem. Mater.* **1995**, *7*, 995. (c) Hu, A.; Ngo, H.; Lin, W. *J. Am. Chem. Soc.* **2003**, *125*, 11490. (d) Hu, A.; Yee, G. T.; Lin, W. *J. Am. Chem. Soc.* **2005**, *127*, 12486. (e) Nonglaton, G.; Benitez, I. O.; Guisle, I.; Pipeler, M.; Leger, J.; Dubreuil, D.; Tellier, C.; Talham, D. R.; Bujoli, B. *J. Am. Chem. Soc.* **2004**, *126*, 1497.

(6) Gopal, K.; Ali, S.; Winpenny, R. E. P. Structural Studies of Paramagnetic Molecular Phosphonates. In *Metal Phosphonate Chemistry: From Synthesis to Applications*; Clearfield, A., Demadis, K., Eds.; Royal Society of Chemistry: Cambridge, U.K., 2012; pp 364−419.

(7) (a) Baskar, V.; Shanmugam, M.; Sañudo, E. C.; Collison, D.; McInnes, E. J. L.; Wei, Q.; Winpenny, R. E. P. *Chem. Commun.* **2007**, 37. (b) Breeze, B. A.; Shanmugam, M.; Tuna, F.; Winpenny, R. E. P. *Chem. Commun.* **2007**, 5185. (c) Khanra, S.; Kloth, M.; Mansaray, H.; Muryn, C. A.; Tuna, F.; Sañudo, E. C.; Helliwell, M.; McInnes, E. J. L.; Winpenny, R. E. P. *Angew. Chem., Int. Ed.* **2007**, *46*, 5568. (d) Baskar, V.; Gopal, K.; Helliwell, M.; Tuna, F.; Wernsdorfer, W.; Winpenny, R. E. P. *Dalton Trans.* **2010**, *39*, 4747. (e) Zheng, Y.-Z.; Breeze, B. A.; Timco, G. A.; Tuna, F.; Winpenny, R. E. P. *Dalton Trans.* **2010**, *39*, 6175. (f) Maheswaran, S.; Chastanet, G.; Teat, S. J.; Mallah, T.; Sessoli, R.; Wernsdorfer, W.; Winpenny, R. E. P. *Angew. Chem., Int. Ed.* **2005**, *44*, 5044. (g) Shanmugam, M.; Chastanet, G.; Mallah, T.; Sessoli, R.; Teat, S. J.; Timco, G. A.; Winpenny, R. E. P. *Chem.—Eur. J.* **2006**, *12*, 8777. (h) Brechin, E. K.; Coxall, R. A.; Parkin, A.; Parsons, S.; Tasker, P. A.; Winpenny, R. E. P. *Angew. Chem., Int. Ed.* **2001**, *40*, 2700. (i) Langley, S.; Helliwell, M.; Raftery, J.; Tolis, E. I.; Winpenny, R. E. P. *Chem. Commun.* **2004**, 142. (j) Langley, S. J.; Helliwell, M.; Sessoli, R.; Rosa, P.; Wernsdorfer, W.; Winpenny, R. E. P. *Chem. Commun.* **2005**, 5029. (k) Langley, S.; Helliwell, M.; Sessoli, R.; Teat, S. J.; Winpenny, R. E. P. *Inorg. Chem.* **2008**, *47*, 497. (l) Langley, S.; Helliwell, M.; Sessoli, R.; Teat, S. J.; Winpenny, R. E. P. *Dalton Trans.* **2009**, 3102. (m) Tolis, E. I.; Helliwell, M.; Langley, S.; Raftery, J.; Winpenny, R. E. P. *Angew. Chem., Int. Ed.* **2003**, *42*, 3804. (n) Tolis, E. I.; Engelhardt, L. P.; Mason, P. V.; Rajaraman, G.; Kindo, K.; Luban, M.; Matsuo, A.; Nojiri, H.; Raftery, J.; Schröder, C.; Timco, G. A.; Tuna, F.; Wernsdorfer, W.; Winpenny, R. E. P. *Chem.—Eur. J.* **2006**, *12*, 8961. (o) Khanra, S.; Konar, S.; Clearfield, A.; Helliwell, M.; McInnes, E. J. L.; Tolis, E.; Tuna, F.; Winpenny, R. E. P. *Inorg. Chem.* **2009**, *48*, 5338. (p) Khanra, S.; Helliwell, M.; Tuna, F.; McInnes, E. J. L.; Winpenny, R. E. P. *Dalton Trans.* **2009**, 6166. (q) Zheng, Y.-Z.; Evangelisti, M.; Winpenny, R. E. P. *Chemical Science* **2011**, *2*, 99. (r) Zheng, Y.-Z.; Evangelisti, M.; Winpenny, R. E. P. *Angew. Chem., Int. Ed.* **2011**, *50*, 3692.

(8) (a) Konar, S.; Bhuvanesh, N.; Clearfield, A. *J. Am. Chem. Soc.* **2006**, *128*, 9604. (b) Yao, H.-C.; Wang, J.-J.; Ma, Y.-S.; Waldmann, O.; Du, W.-X.; Song, Y.; Li, Y.-Z.; Zheng, L.-M.; Decurtins., S.; Xin, X.-Q. *Chem. Commun.* **2006**, 1745. (c) Mitkina, T. V.; Lan, Y.; Mereacre, V.; Shi, W.; Powell, A. K.; Rothenberger, A. *Dalton Trans.* **2008**, 1136. (d) Murugavel, R.; Shanmugan, S. *Dalton Trans.* **2008**, 5358. (e) Konar, S.; Clearfield, A. *Inorg. Chem.* **2008**, *47*, 5573. (f) Murugavel, R.; Gogoi, N.; Clérac, R. *Inorg. Chem.* **2009**, *48*, 646. (g) Ma, Y.-S.; Song, Y.; Tang, X.-Y.; Yuan, R.-X. *Dalton Trans.* **2010**, *39*, 6262. (h) Konar, S.; Clearfield, A. *Inorg. Chem.* **2008**, *47*, 3489. (i) Wang, M.; Ma, C.; Wen, H.; Chen, C. *Dalton Trans.* **2008**, 4612. (j) Wang, M.; Ma, C.; Wen, H.; Chen, C. *Dalton Trans.* **2009**, 994.

(k) Li, J.-T.; Ma, Y.-S.; Li, S.-G.; Cao, D.-K.; Li, Y.-Z.; Song, Y.; Zheng, L.-M. *Dalton Trans.* **2009**, 5029. (l) Konar, S.; Clearfield, A. *Inorg. Chem.* **2008**, *47*, 3492.

(9) (a) Chandrasekhar, V.; Kingsley, S. *Angew. Chem., Int. Ed.* **2000**, *49*, 2320. (b) Chandrasekhar, V.; Nagarajan, L.; Gopal, K.; Baskar, V.; Kögerler, P. *Dalton Trans.* **2005**, 3143. (c) Chandrasekhar, V.; Nagarajan, L.; Clérac, R.; Ghosh, S.; Verma, S. *Inorg. Chem.* **2008**, *47*, 1067. (d) Chandrasekhar, V.; Nagarajan, L.; Clérac, R.; Ghosh, S.; Senapati, T.; Verma, S. *Inorg. Chem.* **2008**, *47*, 5347. (e) Chandrasekhar, V.; Senapati, T.; Sañudo, E. C. *Inorg. Chem.* **2008**, *47*, 9553. (f) Chandrasekhar, V.; Senapati, T.; Sañudo, E. C.; Clérac, R. *Inorg. Chem.* **2009**, *48*, 6192. (g) Chandrasekhar, V.; Nagarajan, L. *Dalton Trans.* **2009**, 6712. (h) Chandrasekhar, V.; Sasikumar, P.; Senapati, T.; Dey, A. *Inorg. Chim. Acta* **2010**, *363*, 2920. (i) Chandrasekhar, V.; Senapati, T.; Dey, A.; Sañudo, E. C. *Inorg. Chem.* **2011**, *50*, 1420.

(10) (a) *Vogel's Text Book of Practical Organic Chemistry*, 5th ed.; Furniss, B. S., Hannaford, A. J., Smith, P. W. G., Tatchell, A. R., Eds.; ELBS and Longman: London, U.K., 1989. (b) Williams, D. B. G.; Lawton, M. *J. Org. Chem.* **2010**, *75*, 8351. (c) Crofts, P. C.; Kosolapoff, G. M. *J. Am. Chem. Soc.* **1953**, *75*, 3379. (d) Bardwell, D. A.; Jeffery, J. C.; Jones, P. L.; McCleverty, J. A.; Ward, M. D. *J. Chem. Soc., Dalton Trans.* **1995**, 2921.

(11) (a) Mukherjee, J.; Mukherjee, R. *Dalton Trans.* **2006**, 1611. (b) Hu, T.-L.; Li, J.-R.; Liu, C.-S.; Shi, X.-S.; Zhou, J.-N.; Bu, X.-H.; Ribas, J. *Inorg. Chem.* **2006**, *45*, 162.

(12) (a) *SMART & SAINT Software Reference Manuals*, version 6.45; Bruker Analytical X-ray Systems, Inc.: Madison, WI, 2003. (b) Sheldrick, G. M. *SADABS a Software for Empirical Absorption Correction*, version 2.05; University of Göttingen: Göttingen, Germany, 2002. (c) Sheldrick, G. M. *SHELXTL*, version 6.12; Bruker AXS Inc.: Madison, WI, 2001. (d) Sheldrick, G. M. *SHELXL97, Program for Crystal Structure Refinement*; University of Göttingen: Göttingen, Germany, 1997. (e) Spek, A. L. *PLATON*; University of Utrecht: Utrecht, The Netherlands, 2001.

(13) Coxall, R. A.; Harris, S. G.; Henderson, D. K.; Parsons, S.; Tasker, P. A.; Winpenny, R. E. P. *J. Chem. Soc., Dalton Trans.* **2000**, 2349.

(14) (a) Singh, A.; Ramanan, A.; Bandyopadhyay, D. *Cryst. Growth Des.* **2011**, *11*, 2743. (b) Ramanan, A.; Whittingham, M. S. *Cryst. Growth Des.* **2006**, *6*, 2419.

(15) (a) An, Y.; Tong, M.-L.; Ji, L.-N.; Mao, Z.-W. *Dalton Trans.* **2006**, 2066. (b) Srivatsan, S. G.; Parvez, M.; Verma, S. *J. Inorg. Biochem.* **2003**, *97*, 340.